Journal of Molecular Structure 1134 (2017) 851–862

Contents lists available at ScienceDirect

Journal of Molecular Structure

journal homepage: http://www.elsevier.com/locate/molstruc

Synthesis, characterization, DFT calculations and biological studies of Mn(II), Fe(II), Co(II) and Cd(II) complexes based on a tetradentate ONNO donor Schiff base ligand

Laila H. Abdel-Rahman*, Nabawia M. Ismail, Mohamed Ismael, Ahmed M. Abu-Dief, Ebtehal Abdel-Hameed Ahmed

Chemistry Department, Faculty of Science, Sohag University, 82524 Sohag, Egypt

ARTICLE INFO

Article history:
Received 16 October 2016
Received in revised form
6 January 2017
Accepted 9 January 2017

Keywords:
Arenes
Arene complexes
Schiff bases
Quantum chemical calculations
Biological studies

ABSTRACT

This study highlights synthesis and characterization of a tetradentate ONNO Schiff base ligand namely (1, 1′- (pyridine-2, 3-dimethyliminomethyl) naphthalene-2, 2′-diol) and hereafter denotes as "HNDAP" and selected metal complexes including Mn(II), Fe(II), Co(II) and Cd(II) as a central metal. HNDAP was synthesized from 1:2 M ratio condensation of 2, 3-diaminopyridine and 2- hydroxy-1-naphthaldhyde, respectively. The stoichiometric ratios of the prepared complexes were estimated using complementary techniques such as; elemental analyses (-C, H, N), FT-IR, magnetic measurements and molar conductivity. Furthermore, their physicochemical studies were carried out using thermal TGA, DTA and kinetic –thermodynamic studies along with DFT calculations. The results of elemental analyses showed that these complexes are present in a 1:1 metal-to- ligand molar ratio. Moreover, the magnetic susceptibilities values at room temperature revealed that Mn(II), Fe(II) and Co(II) complexes are paramagnetic in nature and have an octahedral (O_h) geometry. In contrast, Cd(II) is diamagnetic and stabilizes in square planar sites. The molar conductivity measurements indicated that all complexes are nonelectrolytes in dimethyl formamide. Spectral data suggested that the ligand is as tetradentate and coordinated with Co(II) ion through two phenolic OH and two azomethine nitrogen. However, for Mn(II), Fe(II) and Cd(II) complexes, the coordination occurred through two phenolic oxygen and two azomethine nitrogen with deprotonation of OH groups. The proposed chemical structures have been validated by quantum mechanics calculations. Antimicrobial activities of both the HNDAP Schiff base ligand and its metal complexes were tested against strains of Gram (-ve) *E. coli* and Gram (+ve) *B. subtilis* and *S. aureus* bacteria and *C. albicans*, *A. flavus* and *T. rubrum* fungi. All the prepared compounds showed good results of inhibition against the selected pathogenic microorganisms. The investigated HNDAP Schiff base complexes showed higher activity and stability than their corresponding HNDAP Schiff base ligand and the highest activity observed for Cd(II) complex. Moreover, the prepared Schiff base ligand and its Mn(II) and Co(II) complexes have been evaluated for their anticancer activities against two cancer cell lines namely; colon carcinoma cells (HCT-116 cell line) and hepatocellular carcinoma (Hep-G2) cell lines The interaction of Mn(II) and Co(II) complexes with calf thymus DNA (CT-DNA) was studied by absorption spectroscopic technique and viscosity measurements. Both complexes showed a successful interaction with CT-DNA *via* intercalation mode.

1. Introduction

Schiff bases are substantial class of organic compounds which play a significant role in the development of coordination chemistry as they can easily form stable complexes with most of transition metals [1–3]. The presence of pyridine ring in the structure of Schiff bases had a considerable interest of many authors as it has a great importance in biological systems. In addition, it has been declared that O–hydroxy aromatic aldehydes in synthesis of Schiff bases are the best models used for studying keto-enol tautomerism

* Corresponding author.
E-mail addresses: lailakenawy@hotmail.com (L.H. Abdel-Rahman), Ahmed_benzoic@yahoo.com (A.M. Abu-Dief).

http://dx.doi.org/10.1016/j.molstruc.2017.01.036
0022-2860/

in liquid and solid states [4]. Moreover, they have motivating characteristics for applications of photochromism and thermochromism in both states [5]. This can be demonstrated on basis of intramolecular hydrogen transfer between the azomethine nitrogen and oxygen of hydroxyl group [6]. Also the involvement of the naphthalene group as a nucleus of aldehydes promotes these properties as it is considered as a fluorophore due to its significant photophysical properties and environmental stability [7]. The synthesis of Schiff bases from 2-hydroxy-1-naphthaldehyde with various primary amines has been widely studied as they are applicable in medicine and the highest stability of the formed complexes. Furthermore, the presence of 2-hydroxy-1-naphthaldehyde as precursor provides appropriate binding sites for coordination with metal ions. So the condensation diamines with hydroxyl aldehydes especially 2-hydroxy-1-naphthaldehyde is the aim of most recent researches [8] as their Schiff bases contain nitrogen and oxygen donor atoms [9]. This class of Schiff bases may behave as bidentate, tridentate, tetradentate or hexadentate donor ligands [10]. Two nitrogen and two oxygen atoms in the structure of Schiff bases provide an interesting mode of coordination with metal ions in four active sites so this type of tetradentate Schiff bases became under discussion of many authors [11]. The chemical stability of Schiff base complexes can be affected by the presence of azomethine linkage which has a great importance in increasing the basicity of each nitrogen atom [12]. Schiff bases play a vital role in different applications as antibacterial and antifungal agents alongside other biological applications. Schiff base complexes with ONNO donor atoms are subjected to great studies as oxygen carriers and modeling of bioinorganic processes.

Extensive discussions were reported for Co(II) and Mn(II) complexes with tetradentate Schiff bases with two nitrogen and two oxygen donor atoms as oxygen carriers and catalysts for water-splitting systems. Complexation of Fe(II) with tetradentate ONNO donor Schiff bases in an O_h geometry and the presence of different pyridine derivatives as ligands in the axial position showed spin transition properties [13]. The reported studies revealed that pyridine derivatives have acquired a deal of attention for using them in several applications as in the medicinal and synthesis of organic compounds. The most important applications of some pyridine derivatives included their possible uses as bactericides, fungicides and anticancer agents [14]. It is well known that DNA has a massive importance as it carries all genetic informations of cellular life, so the interaction of Schiff base complexes with DNA gained a special interest due to their applications as cancer therapy agents and different uses in molecular biology [15,16,27]. Schiff base complexes have the ability of cleaving DNA in presence of visible light irradiation in addition to uses in photodynamic therapy of cancer [17]. In the current study we highlight the preparation and characterization of a tetradentate ligand derived from 1:2 M ratio condensation of 2, 3-diaminopyridine and 2-hydroxy-1-naphthaldhyde, respectively in ethanol. Then new complexes of Mn(II), Fe(II), Co(II) and Cd(II) were prepared. The synthesis method of the Schiff base ligand was sufficient for achieving a large yield of the Schiff base ligand. Moreover, using piperidine as a catalyst accelerates the condensation reaction between the starting materials. In our work, we used the reported method for the synthesis of all complexes with fixed conditions suitable for our preparation and this method proved a high efficiency. The structures of prepared complexes were elucidated using complementary spectroscopic and structural techniques. To better understanding the structure actively correlation DFT calculations were performed. The antimicrobial activity of the prepared complexes were tested towards some pathogenic strains of bacteria including Gram positive and Gram negative types besides some species of pathogenic fungi. The cytotoxicity of Mn(II) and Co(II) complexes was also evaluated against two cancer cell lines; colon carcinoma cells (HCT-116 cell line) and hepatocellular carcinoma (Hep-G2) cell lines along with their interaction with DNA that was investigated by means of electronic absorption spectra and viscosity measurements.

2. Experimental

2.1. Materials and instruments

All chemicals, solvents and the metal salts ($MnCl_2 \cdot 4H_2O$, $(NH_4)_2Fe(SO_4)_2 \cdot 6H_2O$, $CoCl_2 \cdot 6H_2O$ and $Cd(NO_3)_2 \cdot 4H_2O$) are of analytical reagent grade and used as received. 2-hydroxy-1-naphthaldhyde is Sigma Aldrich while 2,3-diaminopyridine is Merck grade. Calf thymus DNA (CT-DNA) and Tris [hydroxymethyl]-amino methane (Tris) were obtained from Sigma-Aldrich Chemie. Gallenkamp (UK) apparatus was used for recording melting points of all synthesized compounds. Perkin-Elmer model 240c elemental analyzer was used to collect micro analytical data (C, H, N). Infrared spectra of the synthesized ligand and its metal complexes were recorded on FT-IR Alpha Bruker with Platinum -Ate with KBr pellets in a range of 400–4000 cm^{-1} with a resolution of 4 cm^{-1}. Bruker Biospin NMR spectroscopy magnet system model 400 MHz was used for recording ^{1}HNMR of the ligand with deuterated dimethyl sulfoxide (DMSO) as solvent. Jenway conductivity/TDS meter model 4510 is the system used for molar conductivity measurements of 10^{-3} M of the metal complexes in DMF at room temperature. The magnetic susceptibilities of the complexes were recorded on Gouy's balance and the diamagnetic corrections were made by Pascal's constants and $Hg[Co(SCN)_4]$ for calibration [18]. The absorbance of 1×10^{-3} M for Mn(II), Fe(II) and Cd(II) complexes and 1×10^{-4} for Co(II) complex were determined at various pH levels. A series of Britton universal buffer were used for checking the pH levels [19]. The pH measurements were carried out using HANNA 211 pH meter. All thermogravimetric analyses were performed using Shimadzu cooperation 60H analyzer under a flow of nitrogen

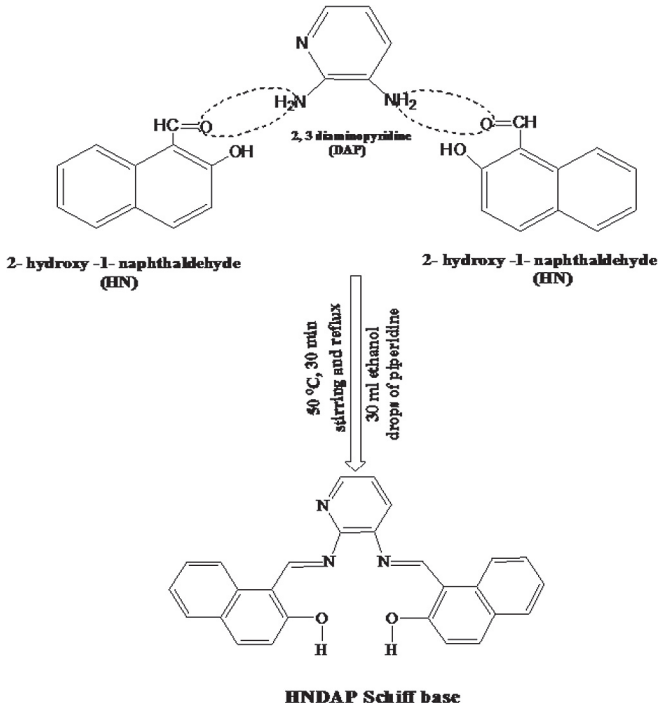

Scheme 1. Synthesis of HNDAP (1, 1′-(pyridine-2, 3-dimethyliminomethyl) naphthalene-2, 2′-diol)) Schiff base ligand.

gas (40 mL/min) with heating rate 5 °C min^{-1} from ambient temperature up to 750 °C. All antimicrobial measurements were estimated in botany department, Faculty of science, Assuit University. Viscosity measurements were performed using Ostwald viscometer immersed in a thermostated water bath maintained at 25 °C.

overnight. During the incubation period the organisms are affected by diffusion of the test solution. After incubation period, the inhibition zones in mm were measured then the activity index was calculated according to the following relation **(1).**

$$\%\ \text{Antimicrobial activity index} = \frac{\text{Inhibition zone of the tested compound(mm)}}{\text{Inhibition zone of standard(mm)}} \times 100 \quad (1)$$

2.2. Synthesis

2.2.1. Synthesis of Schiff base

Scheme 1 shows the synthetic route of HNDAP Schiff base ligand by mixing 0.545 g of 2, 3-diaminopyridine (5 mmol) with 1.72 g of 2-hydroxy-1-naphthaldhyde (10 mmol) in 30 mL ethanol with continuous stirring and reflux for half an hour at 50 °C with the addition of drops of piperidine as a catalyst till the formation of yellow precipitate. The precipitate was then filtered, washed and dried in vacuo over anhydrous $CaCl_2$.

For HNDAP, Yellow color; m. p 260 °C; yield (87%). ^{1}HNMR (400 MHz, DMSO-d_6): δ = 6.92–8.69 (ArH, m, 15H), 9.81 (CH=N, s 1H), 10.03 (CH=N, s, 1H), 14.36 (OH, s, 1H), 15.12 (OH, s, 1H).

2.2.2. Synthesis of Schiff base complexes

(1 mmol, 0.417 g) of the HNDAP Schiff base was mixed with equimolar amounts of metal salts $MnCl_2 \cdot 4H_2O$ (1 mmol, 0.197 g), $(NH_4)_2Fe(SO_4)_2 \cdot 6H_2O$ (1 mmol, 0.392 g), $CoCl_2 \cdot 6H_2O$ (1 mmol, 0.237 g) and $Cd(NO_3)_2 \cdot 4H_2O$ (1 mmol, 0.308 g), respectively in separate flasks each contains 20 mL ethanol. The solution mixtures were stirred magnetically with the addition of a few drops of glacial acetic acid in case of Fe(II) complex to prevent oxidation [20]. After 3 h all complexes were separated, filtered, washed with ethanol, left for drying in vacuo under anhydrous calcium chloride and finally subjected to different types of analyses. Scheme 2 illustrates the synthetic routes and final structures of all synthesized complexes.

2.3. DFT calculations and molecular modeling

Theoretical calculations for all HNDAP ligand and its Cd and Co complex models were performed on Gaussian03 package [21] at density functional theory (DFT) level of theory. Calculations were carried out using 6-31G(d, p) [22] basis set for L3 atoms, and LANL2DZ [23] basis set with effective core potential (ECP) for metal ions.

2.4. Bioassay of the prepared complexes

2.4.1. Antimicrobial activity

2.4.1.1. Antibacterial activity. Determination of antibacterial activity is an extremely important approach for evaluating the efficiency of compounds as antibiotic agents. An in vitro antibacterial activities of the prepared HNDAP Schiff base ligand and its complexes were screened against three types of bacteria *E. coli*, *B. subtilis* and *S. aureus* by disc diffusion method at two concentrations (10 and 20) mg/mL [24, 25]. In this method tetracycline is used as standard and dimethyl sulphoxide (DMSO) as controlling solvent. Sterilized discs with agar as medium wiped with bacterial culture and filled with the test solution. Incubation of plates performed at 37 °C for

2.4.1.2. Antifungal activity. Disc diffusion method is used as an appropriate way for screening the antifungal activity of both HNDAP Schiff base ligand and its complexes against three types of pathogenic fungi *C. albicans*, *A. flavus* and *T. rubrum*. Evaluation of fungicidal activity of all compounds was performed using Fluconazole as standard and dimethyl sulphoxide as a solvent. The used discs have 5 mm in diameter and 1 mm in thickness, filled with the test solution and incubated for three days at 37 °C. Diffusion of the test solution occurred during the incubation time and affected on the growth of pathogenic fungi. Inhibition zone diameter was measured after 36 h of incubation at 37 °C and the activity index of the compounds was determined using the previous mentioned relation **(1).**

2.4.2. Anticancer activity evaluation

HNDAPCo and HNDAPMn complexes were subjected to an evaluation as anticancer agents against two different types of cancer cell lines; colon carcinoma cells (HCT-116 cell line) and hepatocellular carcinoma (Hep-G2) cell lines were obtained from the National Cancer Institute, Cancer Biology Department, Pharmacology Department, Cairo University. The Sulfo-Rhodamine-B-stain (SRB) is the technique used for estimation of the in vitro cytotoxicity of both Co(II) and Mn(II) complexes [14,26,27]. In atypical presented method 96 multi well plates (104 cell/well) were used for saving the cancer cells for 24 h before testing the effect of the prepared complexes to allow the attachment of the cell to the wall of the plate. Different concentrations of the two investigated complexes (0, 1.65, 3.125, 6.25, 12.5, 25 and 50 μM) were prepared in DMSO and added to the cancer cells. The plates were incubated for 48 h at 37 °C then the cells were fixed, rinsed stained with Sulfo-Rhodamine-B-stain. Acetic acid and Tris EDTA buffer were used for washing the excess stain and treatment of the other attached. Then, IC_{50} was evaluated for the tested compounds.

2.4.3. DNA binding experiments

2.4.3.1. Absorption spectral studies. The electronic absorption spectra of Mn(II) and Co(II) complexes were monitored before and after addition of CT-DNA at pH = 7.2 and using Tris-HCl buffer. In the current method a definite concentration of the investigated complex was titrated with incremental amounts of DNA over the range (30–150 μM). The values of intrinsic binding constant for the interaction of the complexes with CT-DNA were calculated from equation (2) [28].

$$[\text{DNA}]\big/\left(\varepsilon_a - \varepsilon_f\right) = \left[[\text{DNA}]\big/\left(\varepsilon_b - \varepsilon_f\right)\right] + 1\big/\text{Kb}\left(\varepsilon_b - \varepsilon_f\right) \quad (2)$$

where, ε_a, ε_f and ε_b are the extinction coefficients observed for the apparent, free and bound complexes, respectively. K_b is the intrinsic binding constant and [DNA] is the concentration in nucleotides.

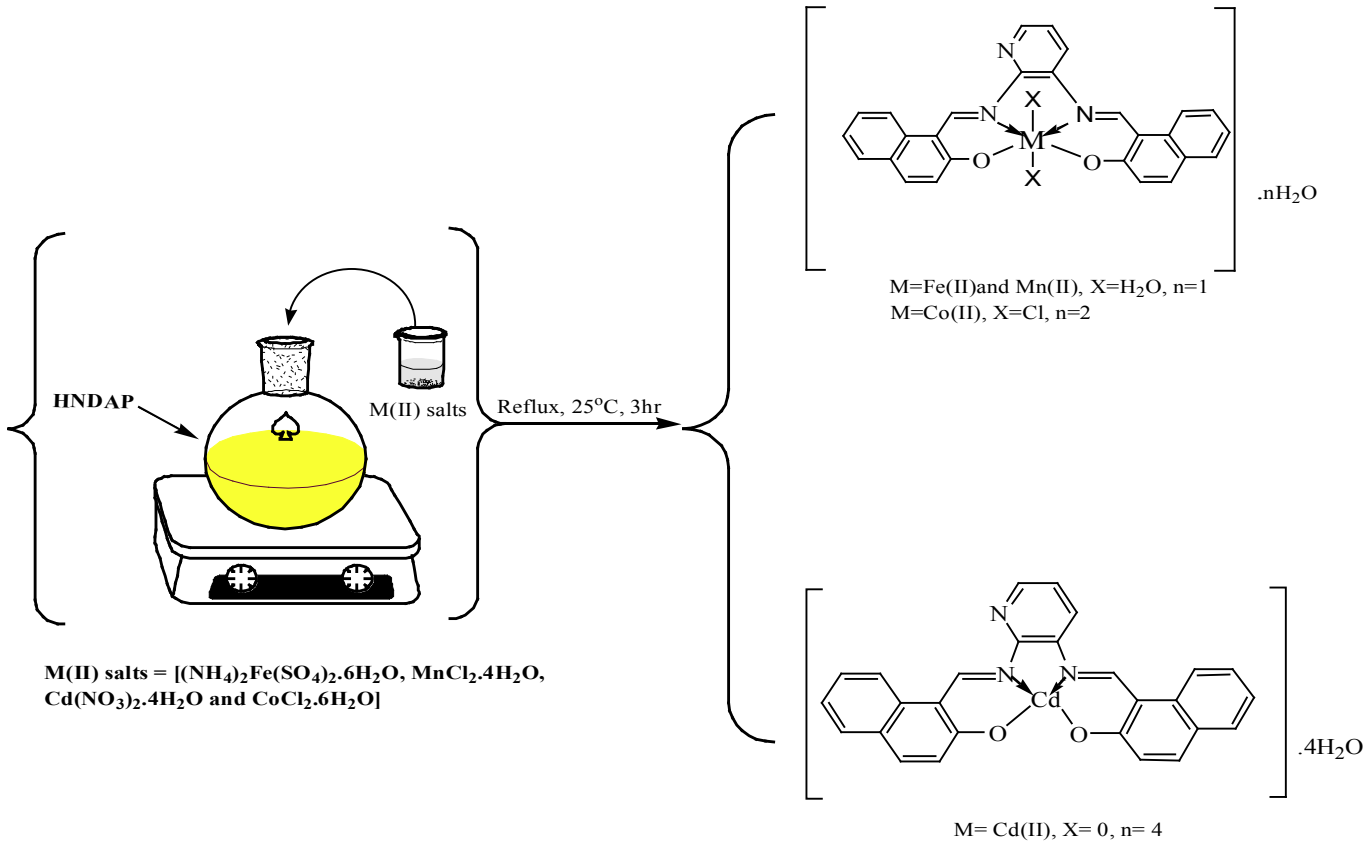

Scheme 2. Synthesis and structures of HNDAP Schiff base complexes.

From the linear relation of $[DNA]/(\varepsilon_a - \varepsilon_f)$ versus [DNA], the k_b was calculated as a ratio of the slope to the intercept.

2.4.3.2. Viscosity measurements. In the present methodology different concentrations of the tested complexes (10–250 μM) were added to DNA with a fixed concentration (250 μM) in an Oswald micro-viscometer immersed in a thermostated water bath at constant temperature 25 °C ± 1. After each successive addition of the complex, the mixture was left for 10 min at 37 °C and the flow time of solutions through the capillary was detected using digital stop watch. For obtaining the concurrent values the experiment was repeated over three times and the results were obtained in the form of $(\eta/\eta^o)^{1/3}$ versus binding mole ratio R (R = [complex]/[DNA]) [29], where η is the viscosity of DNA in the presence of the complex and η^o is that of DNA alone. The relative viscosities of DNA were determined using the relation $\eta = (t - t^o)/t^o$, where t is the observed flow time of DNA containing solution and t^o is the flow time of buffer only.

3. Results and discussion

3.1. Elemental analysis

The percent of carbon, hydrogen and nitrogen for HNDAP Schiff base ligand and its complexes was determined by elemental analyses. From the obtained results in Table 1, all compounds showed a good agreement with the calculated percent values and suggested a 1:1 metal-to -ligand stoichiometric ratio for all prepared complexes.

3.2. IR spectral studies

The infrared (IR) spectra have an important role for identifying the functional groups of the ligand alongside its significant evidence for the interaction between those groups and the central metal ions of the prepared complexes. The IR spectrum of HNDAP Schiff base ligand showed a band at 3427 cm^{-1} which is attributed

Table 1
Analytical and physical measurements of HNDAP Schiff base ligand and its complexes.

Compound	Empirical formula (molecular weight)	Color & Yield (%)	(m.p &d.p) °C	Elemental analysis (Calc%) Found			Molar conductance μS	μ_{eff} (B.M)
				C	H	N		
HNDAP	$C_{27}H_{19}N_3O_2$ (417.49)	Yellow (87)	260	(77.60) 77.21	(4.55) 4.32	(10.06) 9.81	–	–
HNDAPMn	$Mn[C_{27}H_{21}N_3O_4]\cdot H_2O$ (524.39)	Black (75)	>300	(61.78) 61.63	(4.24) 4.70	(8.00) 7.73	19.03	5.81
HNDAPFe	$Fe[C_{27}H_{21}N_3O_4]\cdot H_2O$ (525.49)	Brown (80)	>300	(61.65) 61.30	(4.37) 4.60	(7.99) 7.81	11.24	4.20
HNDAPCo	$Co[C_{27}H_{19}N_3O_2(Cl)_2]\cdot 2H_2O$ (582.39)	Brown (82)	>300	(55.63) 55.42	(3.94) 3.38	(7.21) 6.95	16.40	2.57
HNDAPCd	$Cd[C_{27}H_{17}N_3O_2]\cdot 4H_2O$ (599.89)	Pale brown (86)	>300	(54.00) 53.81	(4.16) 4.43	(7.00) 6.83	9.50	dia

Table 2
IR spectral bands (cm^{-1}) of the HNDAP Schiff base ligand and its complexes.

Compound	$V_{(OH)}$	$V_{(Ar\text{-}CH)}$	$^{V}_{(C=N)}$ Azomethine	$V_{(M\text{-}O)}$	$V_{(M-N)}$
HNDAP	3427(w)	3057(w)	1623(s)	–	–
HNDAPMn	3384(b)	3041(w)	1612(s)	563(w)	503(w)
HNDAPFe	3431(b)	3154(w)	1600(s)	550(w)	499(w)
HNDAPCo	3355(b)	3030(w)	1640(s)	562(w)	504(w)
HNDAPCd	3424(b)	3058(w)	1584(s)	530(w)	476(w)

b = broad, w = weak, s = sharp.

Table 3
The formation constants (K_f), stability constants (pK) and Gibbs free energy (ΔG^*) for HNDAP Schiff base ligand and its complexes in DMF at 298 K.

Complex	Type of the complex	K_f	$_pK_f$	ΔG^* (KJ/mole)
HNDAPMn	1:1	2.20×10^4	4.34	−24.77
HNDAPFe	1:1	1.26×10^6	6.10	−34.80
HNDAPCo	1:1	2.78×10^5	5.44	−31.05
HNDAPCd	1:1	6.00×10^6	6.78	−38.66

to the vibration of phenolic OH group. The characteristic absorption band at 1623 cm^{-1} is due to azomethine linkage [30] which indicated a successful condensation reaction and formation of the Schiff base. Furthermore, the spectrum of the Schiff base ligand exhibits an additional band at 3057 cm^{-1} which assigned to aromatic CH. The comparative infrared spectra of the Schiff base complexes showed a broad band at 3355 - 3431 cm^{-1}. This band may be due to the OH group of lattice or coordinated water molecules [31]. The band of the azomethine linkage of the Schiff base ligand was shifted to different frequencies (1584-1640 cm^{-1}) due to complexation with the metal ion *via* azomethine nitrogen [32]. The spectra of the Schiff base complexes also displayed a weak band at 3041 - 3058 cm^{-1} consistent with aromatic CH. Two new weak bands appeared at lower frequencies at 476 - 504 cm^{-1} and 530 - 563 cm^{-1}, which associated with metal to nitrogen and metal to oxygen bonds, respectively [26]. The infrared spectra for HNDAP Schiff base ligand and its metal complexes are summarized in Table 2.

The proton NMR results for HNDAP Schiff base ligand showed two signals for the hydroxyl groups at 14.36–15.12 ppm. Two signals of azomethine –CH=N– linkages were found at 9.81 ppm and 10.03 ppm. Multiple signals appeared in the range of 6.91–8.69 ppm were assigned to the proton of the aromatic CH [33]. A complete condensation occurred between the amino and carbonyl groups of the used aldehyde which was confirmed by absence of signals from amino groups [34].

3.3. Molar conductivity and magnetic measurements

Conductivity measurements of the prepared complexes were measured in DMF. The values of molar conductivities of 10^{-3} M of the synthesized complexes were in the range of 9.5–19.03 μS at room temperature revealed their non-electrolyte nature [35] and indicated the absence of ions outside coordination sphere [36]. Magnetic susceptibilities of HNDAP Schiff base complexes were measured at room temperature and their calculations were made using the data of diamagnetic corrections and Pascal's constants according to equation (3). The results in Table 1 supported that both Mn(II), Fe(II) and Co(II) have values of effective magnetic moment sufficient for O_h while Cd(II) complex is diamagnetic which determined the d^{10} electronic configuration of Cd (II) and stabilizes in a square planar structure.

$$\mu_{eff} = 2.83\sqrt{X'm*T} \quad X'm = Xm - (\text{diamag. corr}) \tag{3}$$

where, μ_{eff}, T and X′m are the effective magnetic moment (in Bohr Magneton) BM, temperature (K) and is the molar magnetic susceptibility after correction, respectively.

3.4. Estimation of the stoichiometry of the Schiff base complexes

Molar ratio and continuous variation are the simplest spectrophotometric methods for studying the equilibria in solution of Schiff base complexes [37–41]. Application of continuous variation method showed that all HNDAP Schiff base complexes possess as 1:1 metal-to -ligand ratio which confirmed by molar ratio as shown in Fig. 1. Formation constants K_f and Gibbs free energy were calculated using equation (4) and the data were listed in Table 3.

$$K_f = \frac{A/A_m}{C(1 - A/A_m)^2} \text{ in case of } 1:1 \text{ complexes} \tag{4}$$

where, A_m is the absorbance of the maximum formation of the complex, A is the arbitrary chosen absorbance values on either sides of the absorbance mountain col (pass) and C is the initial concentration of the metal. The results revealed that all complexes have relatively high values for formation constant and the stability of

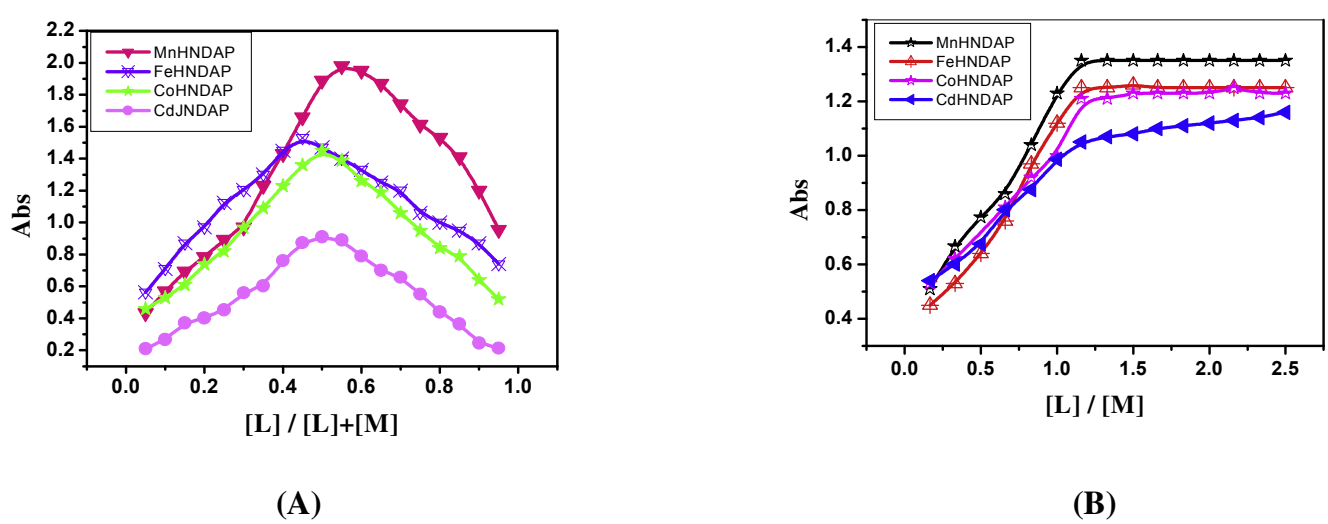

Fig. 1. A representative diagrams of Continuous variation (A) and molar ratio (B) for HNDAP Schiff base complexes in DMF at 10^{-4} M and 298 K.

complexes increased in the following order HNDAPMn < HNDAPCo < HNDAPFe < HNDAPCd. The negative values of Gibbs free energy suggest a spontaneous and favorable reaction.

3.5. Evaluation of stability of the investigated complexes

The investigated complexes exhibited a wide range of stability according to their pH profiles (Fig. 2). The stability for HNDAPMn was in the range (6–10) while both HNDAPFe and HNDAPCd showed high stability over the range (5–10). HNDAPCo was with the highest stability in the range (4–10). The wide range of stability indicates that the condensation reaction with the metal ion greatly stabilizes the Schiff base ligand beside to the possibility of using the synthesized complexes in different physiological reactions.

3.6. Thermal studies

The thermal decomposition pathway of each complex took place at several steps as shown below.

-Thermal decomposition of Mn(II) complex.

$$[C_{27}H_{19}N_2O_2Cd\,].4H_2O \xrightarrow[-4H_2O]{60\,^oC - 250\,^oC} [C_{27}H_{19}N_2O_2Cd] \xrightarrow[-C_5H_3N]{251\,^oC - 475\,^oC} C_{22}H_{14}N_2O_2Cd \xrightarrow[-C_{22}H_{14}ON_2]{475\,^oC - 733\,^oC} CdO$$

-Thermal decomposition of Fe(II) complex.

$$[C_{27}H_{19}N_2O_2Co(Cl)_2].2H_2O \xrightarrow[-2H_2O]{43\,^oC - 242\,^oC} [C_{27}H_{19}N_2O_2Co(Cl)_2] \xrightarrow[-C_{11}H_8ON]{243\,^oC - 499\,^oC} C_{16}H_{15}ON_2Co(Cl)_2 \xrightarrow[-C_{16}H_8ON_2]{500\,^oC - 743\,^oC} CoCl_2$$

-Thermal decomposition of Co(II) complex.

$$[C_{27}H_{19}N_2O_2Mn(H_2O)_2].H_2O \xrightarrow[-H_2O]{35\,^oC - 119\,^oC} [MnC_{27}H_{19}N_2O_2(H_2O)_2] \xrightarrow[-2H_2O]{120\,^oC - 182\,^oC} [C_{27}H_{19}N_2O_2Mn] \xrightarrow[-C_{11}H_7O]{183\,^oC - 310\,^oC} C_{16}H_{10}ON_3 \xrightarrow[-C_5H_3N_3]{311\,^oC - 435\,^oC} C_{11}H_7 \xrightarrow[-C_{11}H_7]{436\,^oC - 680\,^oC} MnO$$

-Thermal decomposition of Cd(II) complex.

$$[C_{27}H_{19}N_2O_2Fe(H_2O)_2].H_2O \xrightarrow[-2H_2O]{33\,^oC - 192\,^oC} [C_{27}H_{19}N_2O_2Fe(H_2O)] \xrightarrow[-H_2O]{193\,^oC - 274\,^oC} [C_{27}H_{19}N_2O_2Fe] \xrightarrow[-C_5H_3N_3]{275\,^oC - 398\,^oC} C_{22}H_{14}O_2Fe \xrightarrow[-C_{22}H_{14}O]{400\,^oC - 601\,^oC} FeO$$

The thermal activation energies and Arrhenius constant of complexes were calculated using Coats and Redfern equation (5). Furthermore, All thermo-kinetic parameters were determined and summarized in Table 4.

$$\log\left[\frac{AR}{\phi E^*}\left(1-\frac{2RT}{E^*}\right)\right]-\frac{E^*}{2.303RT}=\log\left[\frac{\log(W\infty/(W\infty-W))}{T^2}\right] \quad (5)$$

where, W∞ and W are the mass loss at the completion of the decomposition reaction and the mass loss up to temperature T. R and ϕ correspond to the gas constant and the heating rate. The activation energy E*and Arrhenius constant A were obtained from the linear relation between the left hand side of the equation and 1/T since 1 - (2RT/E*) ≈ 1. E* was calculated from the slope with values 0.145, 0.109, 0.190 and 0.092 in KJ mol^{-1} for Mn(II), Fe(II), Co(II) and Cd(II) complexes respectively and Arrhenius constant was obtained from the intercept.

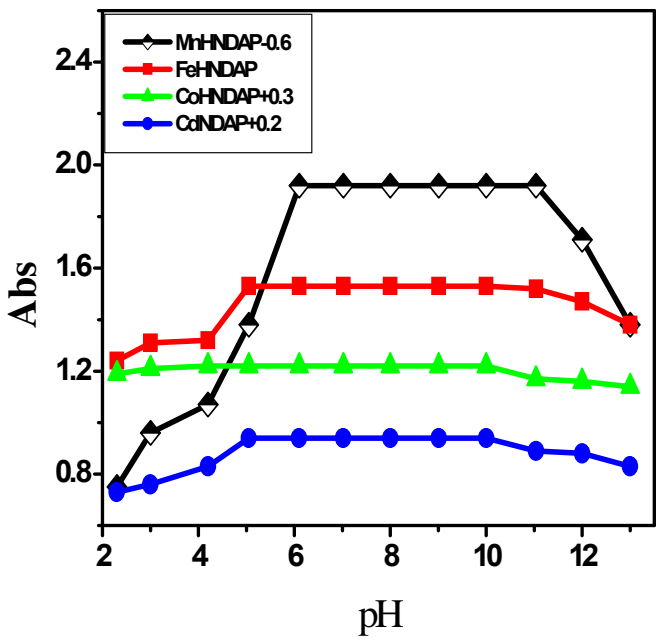

Fig. 2. pH profile of the prepared complexes at [complex] = 1.0 x10^{-3} mol dm^{-3} (except [HNDAPCo] = 1.0 × 10^{-4} mol dm^{-3}) and 298 K.

$$\Delta S^* = 2.303R\log(Ah/KBT)$$
$$\Delta H^* = E^* - RT$$
$$\Delta G^* = H^* - TS^*$$

From the calculated data, we can observe that the entropy of activation values ΔS^* for all complexes are negative in all temperature ranges which revealed the low rate of decomposition reaction. Moreover, this indicates that the activated complex is more ordered than their respective reactants [42]. The positive magnitudes of Gibbs free energy indicate that the decomposition reaction is non-spontaneous in all steps, while the enthalpy of activation of the prepared complexes acquired negative values.

3.7. DFT calculations for the ligand and complex structures

HNDAP molecule was optimized to investigate the geometric and electronic characteristics that may control its electrons donation. Calculations showed that the molecule is planar and four donating groups (2 hydroxyl and 2 imino groups) are facing each other around the central point of the molecule Fig. 3. The structure was found to be stabilized through hydrogen bonding formed between the hydroxyl and imino groups. This specific orientation suggested that the ligand could be bound to the metal ions in one plane, giving raise for the formation of square planar and octahedral geometries for the complexes. The planar geometry was associated with symmetrical charge distribution among the atoms. As can be observed from Fig. 3, the calculated atomic charges the most negative atoms are the oxygen and nitrogen, and the attached protons are the most positive atoms. When moving from the central point the molecule showed more neutral characters. Again this charge distribution supports the idea that the molecule donates the electrons through these four groups. The orbital occupation of highest occupied molecular orbital (HOMO) and lowest unoccupied molecular orbital (LUMO) showed that electrons are delocalized through the whole molecule with calculated energy gap of 8.99 eV.

When optimizing Cd^{2+} ion complex with HNDAP Schiff base ligand, the lowest energy structure has a square planar geometry with molecular formula [HNDAPCd]. This geometry is accomplished with the protonation of the hydroxyl groups to neutralize the Cd^{2+} ion. The stability of this complex came from the formation of two six membered rings between Cd and ligand. Co^{2+} ion formed octahedral [HNDAP$(Cl)_2$Co] complex with HNDAP Schiff base ligand, where the ligand's donor groups coordinated in one plane with addition of two chloride ions bounded in perpendicular plane to HNDAP Schiff base ligand. To prevent the steric effect that occurred between the Co^{2+} and hydroxyl groups of HNDAP, the protons rotated in opposite directions as shown in Fig. 3. When comparing the atomic charge distribution between the two complexes, one can note that in case of Co(II) complex the ligand is more neutral than Cd(II) complex which has more charge interaction between the ligand and the metal than in Co(II) complex, where the ligand has neutral atomic charges (see Fig. 4a and b). Although the optimized structures of Fe^{2+} and Mn^{2+} were octahedral, however the ligand was deprotonated within the coordination and the octahedral geometry was fulfill by two water molecules. Optimization results showed that water molecules coordinated in a plane perpendicular to the M-HNDAP plane Fig. 4c and d. In addition, it has been observed that in both Mn(II) and Fe(II) complexes also the donor groups of the ligand were coordinated with the metal center in one plane.

Table 4
Thermal decomposition steps, mass loss (%), proposed lost segments, final residue and thermo-kinetic activation parameters of HNDAP Schiff base complexes.

Complex	Decomp. Temp (°C)	Mass loss (%) Found (Calc)	Proposed segment	ΔH^* (Kjmol^{-1})	ΔG^* (Kjmol^{-1})	ΔS^* (Jmol^{-1} K^{-1})
HNDAPMn	35–119	4.18 (3.43)	H_2O (hydrated)	−0.86	118	−1.142
	120–182	7.32 (6.86)	$2H_2O$ (coordinated)	−1.22	167	−1.145
	183–310	29.23 (29.74)	$C_{11}H_8O$	−2.01	276	−1.150
	311–435	19.61 (20.02)	$C_5H_3N_3$	−3.77	521	−1.150
	436–680	26.17 (26.50)	$C_{11}H_7$	−5.65	578	−0.156
Residue	>680	13.26 (13.52)	MnO	–	–	–
HNDAPFe	33–192	7.01 (6.85)	$2H_2O$ (hydrated + coordinated)	−1.23	162	−1.107
	193–274	3.50 (3.42)	H_2O (coordinated)	−2.02	278	−1.153
	275–398	19.49 (19.98)	$C_5H_3N_3$	−2.84	393	−1.156
	400–601	56.56 (56.06)	$C_{22}H_{14}O$	−3.81	535	−1.174
Residue	>601	13.44 (13.7)	FeO	–	–	–
HNDAPCo	43–242	7.35 (6.18)	$2H_2O$ (hydrated)	−0.61	83	−1.135
	243–499	29.46 (29.20)	$C_{11}H_8ON$	−1.26	172	−1.140
	500–743	42.37 (42.40)	$C_{16}H_{11}N_2O$	−3.52	483	−1.148
Residue	>743	(22.62) (22.13)	$CoCl_2$ [52]	–	–	–
HNDAPCd	60–250	11.46 (12.00)	$4H_2O$(hydrated)	−1.40	192	−1.149
	251–475	12.71 (12.80)	C_5H_3N	−3.01	415	−1.155
	476–733	53.96 (53.67)	$C_{22}H_{14}ON_2$	−4.43	849	−1.160
Residue	>733	(21.87) (22.00)	CdO	–	–	–

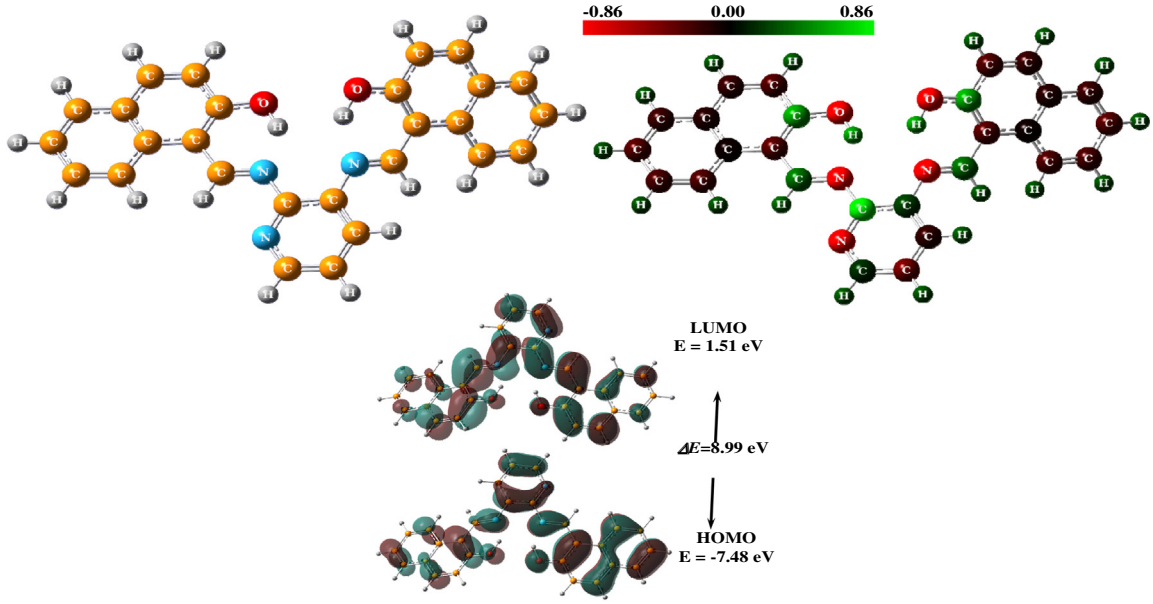

Fig. 3. Optimized structures of HNDAP ligand, atomic charges distributions shown in color range and the HOMO-LUMO orbitals occupation with the calculated energy gap.

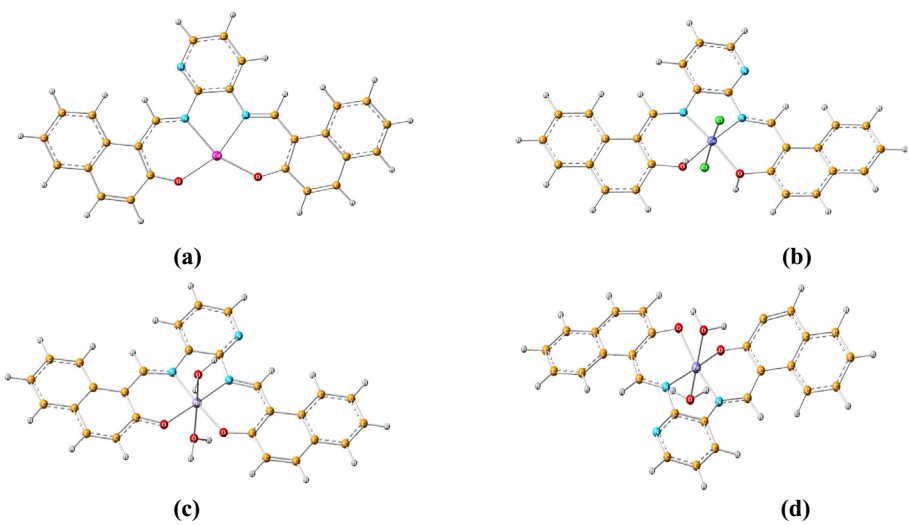

Fig. 4. Optimized structures of (a) [HNDAPCd], (b) [HNDAP(Cl)$_2$Co], (c) [HNDAP(H$_2$O)$_2$Mn] and (d) [HNDAP(H$_2$O)$_2$Fe] complexes.

The relative stability of the prepared HNDAP Schiff base and its complexes in addition to their chemical reactivity were estimated by calculating the universal chemical reactivity descriptors (energy gap, chemical hardness, electronic chemical potential and electrophilicity) Table 5. Chemical hardness (η) is associated with the stability and reactivity of a chemical system. According to frontier molecular orbitals, chemical hardness corresponds to the energy gap between HOMO and LUMO. As the energy gap increases, the molecule becomes harder and more stable/less reactive. The calculated η for the [HNDAP(Cl)$_2$Co] and [HNDAPCd] complexes had insignificant difference. These results suggested that both complexes are relatively stable.

Table 5
Calculated HOMO, LUMO, energy gap (ΔE), chemical hardness (η), electronic chemical potential (μ) and electrophilicity (ω) of the ligand and its corresponding Co(II) and Cd(II) complexes. All values were calculated in eV unit.

Model	HOMO	LUMO	ΔE	η	μ	ω
HNDAP	−7.48	1.51	8.99	4.50	−2.99	0.99
[HNDAP(H$_2$O)$_2$Mn]	−7.43	−1.41	6.02	3.02	−4.42	3.23
[HNDAP(H$_2$O)$_2$Fe]	−8.103	−0.83	7.27	3.63	−4.47	2.75
[HNDAP(Cl$_2$)Co]	−12.82	−10.42	2.40	1.20	−11.62	56.26
[HNDAPCd]	−4.08	−1.61	2.47	1.24	−2.85	3.28

3.8. Antimicrobial activity evaluation of HNDAP Schiff base and complexes

The data of antimicrobial screening are summarized in Tables 6 and 7. Both HNDAP Schiff base ligand and its complexes were tested

Table 6
Antibacterial screening results of HNDAP Schiff base ligand and its complexes.

Compound	Inhibition zone (mm)					
	E. coli (−ve)		*B. subtilis* (+ve)		*S. aureus* (+ve)	
Conc. (mg/mL)	10	20	10	20	10	20
HNDAP	5 ± 0.11	12 ± 0.06	6 ± 0.07	11 ± 0.08	7 ± 0.07	13 ± 0.15
HNDAPMn	7 ± 0.05	19 ± 0.18	10 ± 0.25	23 ± 0.18	13 ± 0.09	24 ± 0.17
HNDAPFe	7 ± 0.23	17 ± 0.17	9 ± 0.06	20 ± 0.24	12 ± 0.13	22 ± 0.05
HNDAPCo	8 ± 0.08	21 ± 0.14	11 ± 0.17	24 ± 0.23	14 ± 0.14	26 ± 0.07
HNDAPCd	11 ± 0.09	24 ± 0.25	15 ± 0.19	28 ± 0.05	18 ± 0.11	33 ± 0.23
Tetracycline	17 ± 0.05	30 ± 0.011	16 ± 0.014	33 ± 0.23	24 ± 0.20	39 ± 0.17

Table 7
Antifungal screening results of HNDAP Schiff base ligand and its complexes.

Compound	Inhibition zone (mm)					
	C. albicans		*A. flavus*		*T. rubrum*	
Conc.(mg/mL)	10	20	10	20	10	20
HNDAP	5 ± 0.09	9 ± 0.23	3 ± 0.11	8 ± 0.07	2 ± 0.19	4 ± 0.16
HNDAPMn	9 ± 0.06	17 ± 0.07	8 ± 0.08	17 ± 0.05	7 ± 0.15	12 ± 0.05
HNDAPFe	8 ± 0.10	15 ± 0.23	7 ± 0.17	13 ± 0.09	6 ± 0.06	10 ± 0.11
HNDAPCo	12 ± 0.08	19 ± 0.09	8 ± 0.26	18 ± 0.25	6 ± 0.09	11 ± 0.18
HNDAPCd	14 ± 0.12	24 ± 0.14	11 ± 0.13	21 ± 0.11	9 ± 0.24	15 ± 0.07
Fluconazole	16 ± 0.16	28 ± 0.25	12 ± 0.09	25 ± 0.07	10 ± 0.22	17 ± 0.15

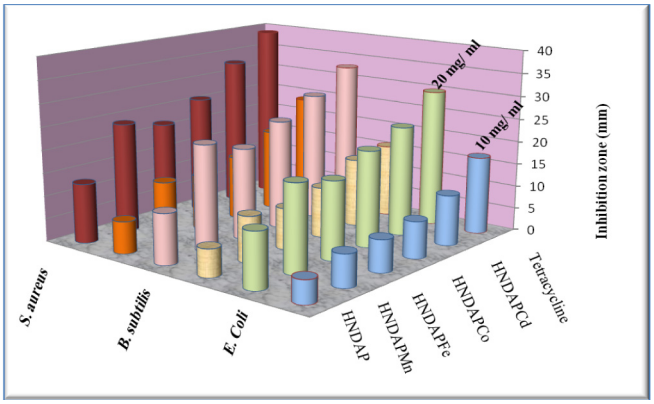

(a)

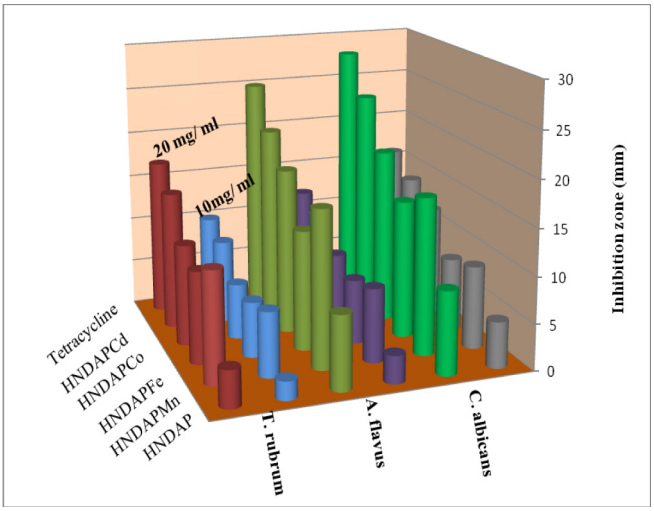

(b)

Fig. 5. a. A histogram show the antibacterial evaluation of the investigated HNDAP Schiff base ligand and its complexes. **b.** A histogram show the antifungal evaluation of the investigated HNDAP Schiff base ligand and its complexes.

for their antibacterial activities against one Gram negative bacteria *E. coli* beside two Gram positive bacteria *B. subtilis* and *S. aureus* Fig. 5(a). Antifungal activities were measured against three different types of pathogenic fungi; *C. albicans*, *A. flavus* and *T. rubrum* Fig. 5b. Both the Schiff base ligand and its complexes exhibited varying degrees of inhibitory effect on the growth of selected microorganisms. The results showed that *B. subtilis* is the most sensitive microorganism to the investigated complexes. From the comparison of the activity of complexes with these of the Schiff base, it seems that all complexes have better values of antibacterial and antifungal activities than their bare Schiff base ligand under the same experimental conditions with the highest antimicrobial activity observed for Cd(II) complex. This could be explained according to the difference in geometry and steric hindrance effect, which facilitates the penetration and inhibition of microorganism's cell. Moreover, it is obvious that there is a direct correlation between the stability of some prepared complexes and their activity against some types of microorganisms. It is obvious from the calculated values of stability constants for the prepared complexes, that their stability increases according to the order HNDAPMn < HNDAPCo < HNDAPFe < HNDAPCd. We can correlate between the stability of HNDAP Schiff base complexes and their activity against different strains of pathogenic microorganisms. It is observed in Cd(II) complex the increased stability may enhance its biological activity.

Overtone's concept and chelation theory have discussed the reason for high antimicrobial activities of Schiff base complexes over their respective Schiff base ligand. It has been reported that on chelation, the polarity of the metal ion can be reduced to a major extent due to the overlap of the ligand orbital and partial involvement of the positive charge of the metal ion with donor groups. Further, it increases the delocalization of π-electrons over the entire chelating ring and enhances the penetration of the complexes into lipid membranes and thus blocking the metal binding sites in the enzymes of microorganisms. There are other factors which may increase the activity such as; solubility, conductivity and bond length between the metal and ligand [43–46]. The minimum inhibition concentration of the HNDAP Schiff base ligand and its complexes was determined by serial dilution method and the results were listed in Table 8.

Table 8
Minimum inhibition concentration in (mg/mL) of HNDAP Schiff base ligand and its metal complexes.

Compound	Bacteria			Fungi		
	E. coli (−ve)	*B. subtilis* (+ve)	*S.aureus* (+ve)	*C. albicans*	*A. flavus*	*T. rubrum*
HNDAP	8.50	8.00	7.50	8.00	8.50	9.00
HNDAPMn	4.00	5.50	6.00	4.00	5.50	6.00
HNDAPFe	6.00	5.00	4.50	5.00	6.00	7.00
HNDAPCo	4.50	4.00	3.00	3.50	5.00	5.50
HNDAPCd	3.00	2.00	1.50	2.00	2.50	3.50

Table 9
Antibacterial and antifungal activity indexes for the synthesized HNDAP Schiff base ligand and its complexes at 20 mg/mL.

Compound	Activity index (%)					
	E. coli (−ve)	*B. subtilis* (+ve)	*S. aureus* (+ve)	*C. albicans*	*A. flavus*	*T. rubrum*
HNDAP	40.00	33.30	33.30	32.14	32.00	23.50
HNDAPMn	63.30	69.70	61.50	60.70	68.00	70.58
HNDAPFe	56.60	60.60	56.40	67.85	72.00	58.80
HNDAPCo	70.00	72.70	67.85	53.57	52.00	64.70
HNDAPCd	80.00	84.80	84.60	85.70	84.00	88.20

The calculation of activity index in Table 9 confirmed the relative antimicrobial activity of the prepared complexes.

3.9. Anticancer activity evaluation

The cytotoxic ability of compounds HNDAP, HNDAPMn, HNDAPCo was evaluated against colon carcinoma cells (HCT-116 cell line) and hepatocellular carcinoma (Hep-G2) cell lines. The in vitro screening of the anticancer activity detected that the investigated compounds have a significant cytotoxicity against HCT-116 and Hep-G2 cell lines. Moreover, the results revealed that both HNDAPMn and HNDAPCo have more anticancer activity than their corresponding HNDAP Schiff base ligand see Fig. 6. It was observed that HNDAPCo is more potent against liver sarcoma cell line (Hep-G2), but HNDAPMn has more cytotoxic activity against colon carcinoma cell line (HCT-116).

3.10. DNA binding studies

3.10.1. Electronic absorption spectra

Measurements of absorption spectra of the investigated complexes in presence of different concentrations of DNA are one of the most significant methods in the determination of interaction of these complexes with CT-DNA [47]. Related to the

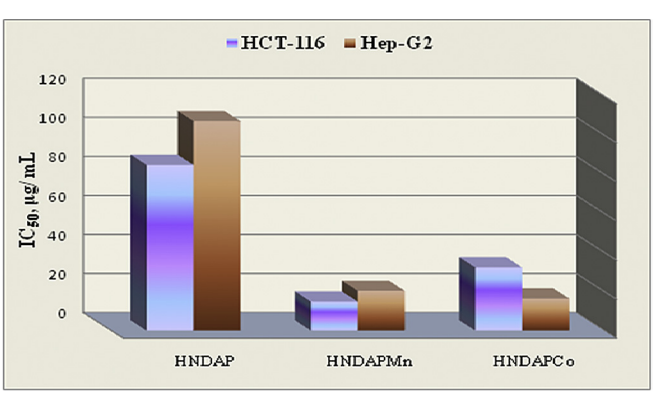

Fig. 6. IC_{50} representation of HNDAP Schiff base ligand and its Mn(II) and Co(II) complexes against colon carcinoma cell line, (HCT-116) and Liver sarcoma cell line (Hep-G2).

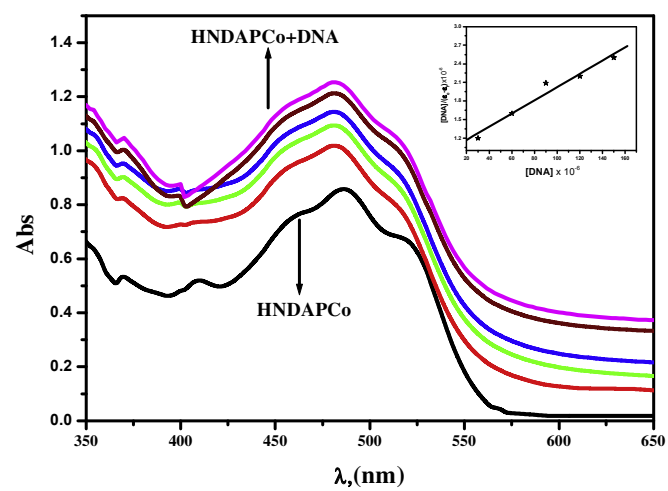

Fig. 7. Absorption spectra of HNDAPCo complex in the absence and presence of increasing DNA, [Co] = 6.6 × 10^{-5}, [DNA] = (30–150 µM) and pH = 7.2. Inset: linear plot for calculating the intrinsic DNA binding constant.

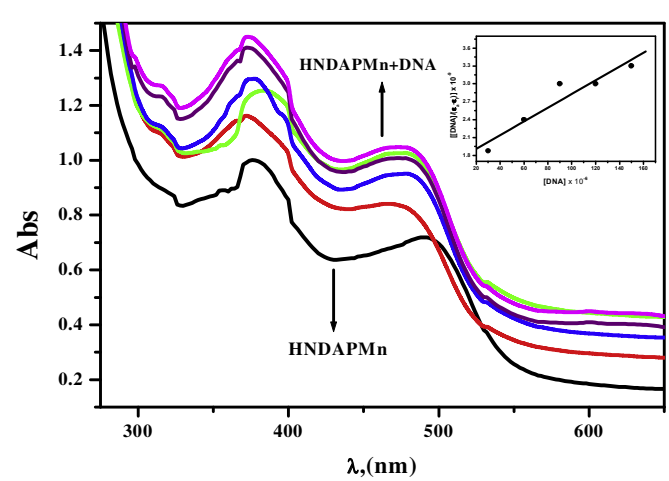

Fig. 8. Absorption spectra of HNDAPMn complex in the absence and presence of increasing DNA, [Mn] = 1 × 10^{-5} M, [DNA]=(30–150 µM) and pH = 7.2. Inset: linear plot for calculating the intrinsic DNA binding constant.

Table 10
Intrinsic binding constant (K_b) and standard Gibb's free energy (ΔG^*) of the prepared Schiff base complexes.

Complex	λ_{max} free (nm)	λ_{max} bound (nm)	Δn	Chromism (%)[a]	Type of Chromism	Binding Constant 10^4 M^{-1}	ΔG^* $KJmol^{-1}$
HNDAPCo	488	484	4.00	18.55	Hyper	1.11	−23.07
HNDAPMn	378	384	6.00	20.00	Hyper	0.68	−21.86
	492	478	14.00	5.00	Hyper		

[a] Chromism (%) = $(A_{free} - A_{bound})/A_{free}$.

double helical structure of CT-DNA, the most considerable spectral effects proceeded in the interaction with Schiff base complexes are hyperchromic and hypochromic [48]. The hyperchromicity feature in DNA binding may be explained based on partial uncoiling of the double helix structure which facilitates the interaction with more bases [49]. The electronic absorption spectra of HNDAPCo and HNDAPMn complexes were carried out at a fixed concentration of the complex 6.6×10^{-5} and 1×10^{-5} respectively see Figs. 7 and 8. The absorbance intensity of the complexes changes with a manifest hyperchromic effect upon the gradual addition of CT-DNA over the range (30–150 μM). For comparing the strength of the interaction the complexes, the intrinsic binding constants were calculated from the plot of linear relation between [DNA]/(ε_a - ε_f) and [DNA], where the values of binding constant can be determined as a ratio of the slope1/(ε_b -ε_f) and intercept 1/K_b (ε_b-ε_f). The results revealed that the complexes are good binders with CT-DNA *via* intercalation mode with an intrinsic binding constants 1.11×10^4 $M^{-1}$and 0.69×10^4 M^{-1} for HNDAPCo and HNDAPMn, respectively. All the values of standard Gibb's free energy and the intrinsic binding constant are summarized in Table 10.

3.10.2. Viscosity measurements

For the determination of the binding mode of DNA, viscosity is the most conclusive and the least obscure method [50]. As the intercalation mode occurs between the DNA molecule and the binder agent, an obvious separation of the base pairs which can be detected by measuring the relative specific viscosity [51–53]. The viscosity data of both HNDAPCo and HNDAPMn complexes increased gradually with variation in the concentration of complexes (Fig. 9) which is a strong evidence for intercalation effect of our investigated complexes with CT-DNA.

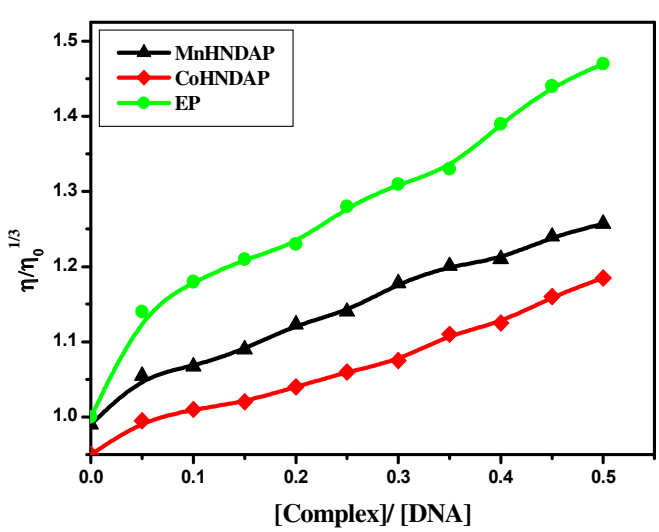

Fig. 9. The effect of increasing the amount of the prepared complexes on the relative viscosities of DNA at [DNA] = 0.5 mM, [complex] and [EB] = 25–250 μM and 298 K.

4. Conclusion

The current framework presents a simple method for the preparation of the Schiff base ligand HNDAP and selected complexes for Fe(II), Mn(II), Co(II) and Cd(II). Both the Schiff base ligand and its complexes were characterized by several physicochemical and spectral analyses for determination of their geometry. The biological assessment of the complexes has been estimated for antimicrobial activity. The complexes exhibited high activity compared to their corresponding Schiff base ligand which indicates that metallization enhances the activity compared of the prepared complexes. In addition, the evaluation of both HNDAP and its Mn(II) and Co(II) as anticancer agents was performed against colon carcinoma (HCT-116 cell line) and hepatocellular carcinoma (Hep-G2) cell lines. The obtained data revealed that the tested complexes have higher anticancer activity than their bare Schiff base ligands and they are relatively potent cancer agents. Furthermore, the interaction with CT-DNA was carried out by means of electronic absorption spectra and viscosity measurements. The investigated complexes for DNA binding ability showed good results in binding *via* intercalation mode. Moreover, the structural characteristics of HNDAP Schiff base ligand and complexes have been investigated using quantum chemical calculations to show the source of the molecular activity.

References

[1] A.A. El-Sherif, T.M.A. Eldebss, Spectrochim. Acta Part A 79 (2011) 1803–1814.
[2] L.H. Abdel Rahman, A.M. Abu-Dief, N.A. Hashem, A.A. Seleem, Int. J. Nano. Chem. 1 (2015) 79–95.
[3] L.H. Abdel-Rahman, A.M. Abu-Dief, M. Ismael, A.A. Mohamed, N.A. Hashem, J. Mol. Struct. 1103 (2016) 232–244.
[4] K. Užarević, M. Rubčić, V. Stilinović, B. Kaitner, M. Cindrić, J. Mol. Struc 984 (2010) 232–239.
[5] P. Fita, E. Luzina, T. Dziembowska, Cz. Radzewicz, A. Grabowska, J. Chem. Phys. 125 (2006) 184508.
[6] Aysel Başoglu, Semanur Parlayan, Miraç Ocak, Hakan Alp, Halit Kantekin, Mustafa Özdemir, Ümmühan Ocak, Polyhedron 28 (2009) 1115–1120.
[7] Elham S. Aazam, JKAU Sci. 22 (2) (2010) 101–116.
[8] P.G. Cozzi, Chem. Soc. Rev. 33 (2004) 410–421.
[9] A.K. Sah, T. Tanase, M. Mikuriya, Inorg. Chem. 45 (2006) 2083–2092.
[10] A. Blagus, B. Kaitner, Acta Crystallogr. C65 (2009) m455–m458.
[11] Zhong Yu, T. Kuroda-Sowa, H. Kume, T. Okubo, M. Maekawa, M. Munakata, Bull. Chem. Soc. Jpn. 82 (2009) 333–337.
[12] K. Jamuna, B.R. Naik, B. Sreenu, K. Seshaiah, J. Chem, Pharm. Res. 4 (9) (2012) 4275–4282.
[13] B. Weber, C. Carbonera, C. Desplances, J.-F. Létard, Eur. J. Inorg. Chem. (2008) 1589–1598.
[14] L.H. Abdel-Rahman, Ahmed M. Abu-Dief, Rafat M. El-Khatib, Shimaa Mahdy Abdel-Fatah, Bioorg. Chem. 69 (2016) 140–152.
[15] A.T. Chaviara, E.E. Kioseoglou, A.A. Pantazaki, A.C. Tsipis, P.A. Karipidis, D.A. Kyriakidis, C.A. Bolos, J. Inorg, Biochem 102 (2008) 1749–1764.
[16] N. Mahalakshmi, R. Rajavel, Inter. J. Pharm. Technol. 2 (4) (2010) 1133–1157.
[17] A.K. Patra, T. Bhowmick, S. Roy, S. Ramakumar, A.R. Chakravarty, Inorg. Chem. 48 (7) (2009) 2932–2943.
[18] L.H. Abdel-Rahman, Rafat M. El-Khatib, Lobna A.E. Nassr, Ahmed M. Abu-Dief, I. Mohamed, A.S. Amin, Spectrochim. Acta 117 (2014) 366–378.
[19] H.T.S. Britton, Hydrogen Ions, third ed.,, Chapman and Hall, London, UK, 1952.
[20] L.H. Abdel-Rahman, Rafat M. El-Khatib, Lobna A.E. Nassr, Ahmed M. Abu-Dief, Fakhr El-Din Lashin, Spectrochim. Acta Part A. Mol. Biomol. Spectrosc. 111 (2013) 266–276.
[21] M.J. Frisch, et al., Gaussian 03, Revision C.01, Gaussian Inc, Wallingford CT, 2004.
[22] R. Ditchfield, W.J. Hehre, J.A. Pople, J. Chem. Phys. 54 (1971) 724–728.
[23] P.J. Hay, W.R. Wadt, J. Chem. Phys. 82 (1985) 270–283.

[24] E.C.S. Chan, M.J. Pelczar, N.R. Krieg, Microbiology, fifth ed., 1998.
[25] A. Wolfe, G.H. Shimer, T. Mechan, Biochemistry 26 (1987) 6392–6396.
[26] L.H. Abdel-Rahman, A.M. Abu-Dief, R.M. El-Khatib, S.M. Abdel-Fatah, J. Photochem. Photobiol. B 162 (2016) 298–308.
[27] A.M. Abu-Dief, I.F. Nassar, W.H. Elsayed, Appl. Organometal. Chem. 30 (2016) 917–923.
[28] L.H. Abdel-Rahman, A.M. Abu-Dief, N.M. Ismail, M. Ismael, Inorg. Nano-Metal Chem. 47 (2017) 467–480.
[29] L.H. Abdel-Rahman, Ahmed M. Abu-Dief, Samar Kamel Hamdan, Amin Abdou-Seleem, Int. J. Nano. Chem. 1 (2) (2015) 65–77.
[30] A.A. Emara, Spectrochim. Acta Part A Mol. Biomol. Spectrosc. 77 (2010) 117–125.
[31] L.H. Abdel-Rahman, A.M. Abu-Dief, E.F. Newair, S.K. Hamdan, J. Photochem. Photobiol. B 160 (2016) 18–31.
[32] Mohammad Nasir Uddin, D.A. Chowdhury, M.D. Moniruzzman Rony, Am. J. Chem. Appl. 1 (2014) 12–18.
[33] Ikechukwu P. Ejidike, Peter A. Ajibade, Molecules 20 (2015) 9788–9802.
[34] R. El-Shiekh, M. Akl, A. Gouda, W. Ali, J. Am. Sci. 7 (4) (2011) 797–807.
[35] A.A.M. Belal, I.M. El-Deen, N.Y. Farid, Rosan Zakaria, Moamen S. Refat, Spectrochim. Acta Part A Mol. Biomol. Spectrosc. 149 (2015) 771–787.
[36] L.H. Abdel-Rahman, Rafat M. El-Khatib, Lobna. A.E. Nassr, Ahmed M. Abu Dief, J. Mole. Struct. 1040 (2013) 9–18.
[37] A.M. Abu-Dief, L.A.E. Nassr, J. Iran. Chem. Soc. 12 (2015) 943–955.
[38] M. Hany, Abd El-Lateef, Ahmed M. Abu-Dief, A.A. Moniur, J. Mol. Struct. 1130 (2017) 522–542.
[39] M. Hany, Abd El-Lateef, Ahmed M. Abu-Dief, Bahaa El-Dien, M. El-Gendy, J. Electroanal. Chem. 758 (2015) 135–147.
[40] M. Hany, Abd El-Lateef, Ahmed M. Abu-Dief, L.H. Abdel-Rahman, Eva Carolina Sañudo, Núria Aliaga-Alcalde, J. Electroanal. Chem. 743 (2015) 120–133.
[41] W.G. Hanna, M.M. Moawad, Tran. Metal. Chem. 26 (2001) 644–651.
[42] G.B. Bagihalli, S.A. Patil, P.S. Badami, J. Iran, Chem. Soc. 6 (2009) 259–267.
[43] V.P. Singh, A. Katiyar, Bio Met. 21 (2008) 491–501.
[44] A.M.N. Khaleel, A.J. Abdul-Ghani, Bioinorganic Chem. Appl. (2013) 1–14.
[45] O.A. El-Gammal, G. Abu El-Reash, S.F. Ahmed, Spectrochim. Acta Part A. Mol. Biomol. Spectrosc. 135 (2015) 227–240.
[46] M. Barwiolek, E. Szlyk, A. Berg, T. Muziol, J. Jeziersk, RSC 43 (2014) 9924–9933.
[47] A. Raja, V. Rajendiran, P.U. Maheswari, R. Balamuugan, C.A. Kilner, M.A. Halcrow, J. Inorg. Biochem. 99 (2005) 1717–1732.
[48] N.Z. Tian, Y. Zhou, S.G. Sun, Y. Ding, L.W. Zhong, Sci. Mag. 316 (2007) 732–735.
[49] G. Pratviel, J. Bernadou, B. Meunier, Adv. Inorg. Chem. 45 (1998) 251–312.
[50] D.D. Li, J.L. Tian, W. Gu, X. Liu, H.H. Zeng, S.-P. Yan, J. Inorg. Biochem. 105 (2011) 894–901.
[51] J. Wang, Z.Y. Yang, X.Y. Yi, B.D. Wang, J. Photochem. Photobiol. A. Chem. 201 (2009) 183–190.
[52] L.H. Abdel-Rahman, R.M. El-Khatib, Ahmed M. Abu-Dief, Shimaa M. Abdel-Fatah, A.A. Sleem, Int. J. Nano.chem. 2 (2016) 83–91.
[53] M. Barwiolek, E. Szlyk, An. Berg, T. Muziol, J. Jeziersk, RSC 43 (2014) 9924–9933.